MLM-1160
TID-4500 (25th Ed.)
Category - UC-2
Progress Reports

MOUND LABORATORY PROGRESS REPORT FOR JUNE, 1963

J. F. Eichelberger
G. R. Grove
L. V. Jones

Date: June 28, 1963

The Mound Laboratory Progress Report, issued monthly, is intended to be a means of reporting items of current technical interest in research and development programs. To issue this report as soon as possible after the end of the month, editorial work is limited; and since this is an informal progress report, the results and data presented are preliminary and subject to change.

These reports are not intended to constitute publication in any sense of the word. Final results either will be submitted for publication in regular professional journals or will be published in the form of MLM topical reports.

The previous reports in this series are: MLM-1146
MLM-1148
MLM-1151
MLM-1152
MLM-1155
MLM-1157

MONSANTO RESEARCH CORPORATION

A SUBSIDIARY OF MONSANTO CHEMICAL COMPANY

MOUND LABORATORY

MIAMISBURG, OHIO

OPERATED FOR

UNITED STATES ATOMIC ENERGY COMMISSION

U.S. GOVERNMENT CONTRACT NO. AT-33-1-GEN-53

TABLE OF CONTENTS

DISCLAIMER

SUMMARY

Radioelements Research

Half-life of Tritium The half-life of tritium was determined calorimetrically over a 1456-day period. The half-life was calculated to be 12.355 ± 0.010 years, based on measurements in three calorimeters.

Polonium-208 The yields of polonium-208 and polonium-209 from the irradiation of multicurie quantities of polonium-210 were calculated. Production of small quantities of polonium-208 and polonium-209 is possible by the (*n*, *xn*) reaction; however, large quantities of polonium-210 would be present in the polonium-208 polonium-209 sample. On the basis of these calculations the maximum polonium-208 content would occur after 466 days' irradiation in the materials testing reactor.

An experimental decay scheme was drawn for polonium-208 on the basis of present experimental data. Experiments are in progress to determine whether levels at about 1.4 Mev in bismuth-208 are populated in the electron capture decay of polonium-208.

Determination of Coincidence Correction The known half-life method for determining the resolution time of a counting instrument was found to yield only an average value for the counting range in the computation. To correct the counting error a series of computations should be made with data covering only a short segment of the decay curve rather than a single computation covering the entire range. Alternatively, the decaying-pair method of half-life determination can be used, eliminating the need for an accurate knowledge of the resolution time.

Uranium-234 Separation A process for the separation of uranium-234 from plutonium-238 has been developed. One batch of feed solution was processed by the method, and 14 milligrams of uranium-234 were recovered. A second continuous solvent extraction process is being investigated.

Potassium Plutonium Sulfate Dihydrate Thermogravimetric studies and the differential thermal analysis of potassium plutonium sulfate dihydrate have been completed. The previously reported DTA thermogram for salt has been confirmed. The existence of the complex acid $H_4Pu(SO_4)_4$ is indicated.

The solubility of potassium plutonium sulfate dihydrate was determined in solutions of 0.959 molar sulfuric acid containing potassium chloride at concentrations from 0.1 to 0.5 molar. The values were plotted in a straight line with a slope of 4.08, as compared to a theoretical 4.00.

A thermogravimetric analysis of potassium plutonium sulfate dihydrate has been completed. Thermograms of this dihydrate and of plutonium sulfate tetrahydrate indicate that a crystalline phase transformation occurs after the waters of hydration are driven off. The potassium sulfate alpha-to-beta phase transformation was absent from the dihydrate salt thermogram indicating that no free potassium sulfate was present.

Isotope Separation

Carbon-13 Two cascaded, 24-foot, hot-wire thermal diffusion columns are being used to remove heavy gaseous impurities, such as nitrogen, carbon monoxide, and ethane, from 99 per cent pure natural methane. In a three-column series system the carbon-13 content is seven per cent in 89 per cent methane at the bottom of the third stage. The first five stages of a seven-stage thermal diffusion column cascade system enriched natural methane to about ten per cent carbon-13.

Thermal diffusion column transport coefficients are being measured for various carbon monoxide masses, and an accurate value is being determined for the experimental hot wall temperature.

An experimental system is being designed for studying the nonaqueous carbamate chemical exchange method for enriching carbon-13. The system is expected to yield a separation factor up to 1.39, although about 100 hours is required for equilibrium.

Thermal Diffusion The use of alternating current for heating column center wires is being studied. A 36-inch wire was attached to a wooden fram, while the bottom of the wire was allowed to swing freely in a pool of mercury. At 48 amperes and 24 volts the wire was deflected to the side of the mercury container; a larger container lessened the deflection. A magnetic field between the lead wire and the center wire may also increase deflection.

The equation describing the steady state vibrations of column wire heated by alternating current was derived.

Alpha and Neutron Source Development

Alpha Sources To date, the maximum amount of polonium which could be contained by electroplated gold was 5-10 millicuries per square centimeter. By a new procedure the maximum polonium concentration may be increased by several orders of magnitude: freshly electroplated polonium was transferred wet from the polonium plating bath to a silver strike bath and then to a gold plating bath. Experiments to confirm this increase are continuing.

Neutron Sources Two PoBe sources prepared late in 1957 were returned from the Martin-Marietta Corporation. An alpha pulse height analysis of one source showed no peaks characteristic of polonium-208 or -209.

Analytical

Beryllium Analysis by Gamma Activation A new method was developed for the destructive analysis of beryllium. A dissolved beryllium sample was irradiated by an antimony-124 gamma source to cause a (γ,n) reaction. The neutrons activated an indium detector which was then beta counted; the beta count rate is proportional to the neutron flux. The analysis results were an average 0.08 per cent below values obtained by gravimetric analyses.

Low-level Krypton Counting A sample of fission product xenon containing an estimated 10^{-9} atom per cent krypton-85 was counted in the low-level counting system. The results indicated that gases containing less than 10^{-12} atom per cent krypton-85 can be detected in this system; however, krypton is adsorbed on the walls of the proportional counting chamber during an experiment; hence, a purging procedure is being developed to keep the counter background at a constant rate.

Basic and applied research on a number of radioelements is being conducted to determine physical properties, develop analytical techniques, and study the basic radiochemistry involved. Of particular interest are alpha emitters, their decay chains, their isotopes, and their chemical homologs.

Half-life of Tritium The tritium half-life, as determined from a gas and a salt sample were reported previously as 12.352 ± 0.009 (internal probable error) years. The current value of 12.355 years substantiates this value, and the internal probable error has been reduced by a factor of three. After an analysis of the results and comparison with other half-life determinations, an absolute probable error of 0.010 years was assigned (12.355 ± 0.010 years).

Table 1 gives the half-life results from all data taken with Calorimeters 39, 51, and 77. Solutions were obtained by the weighted log method of least squares, i.e., weights were assigned to remove the inherent weighting that occurs in taking the logarithm of each power measurement. Therefore, the solutions are identical to one obtained by the unweighted variation, or general method. Row 1 of Table 1 gives the estimated half-life (12.361 years) from the portion of the Calorimeter 39 data of 553 to 1456 days in which no deviation was apparent. Row 2 gives the solution (12.357 years) from a larger portion of the data including a curvature that may have been caused by slow variations in the calorimeter. Row 3 gives the result (12.345 years) for the borderline case where the curvature in the deviations is somewhat greater than would be expected from slow variations or from chemical activity so long after fabrication of the source. Row 4 gives the results for the entire time span (12.335 years) where the deviations are of such magnitude that they can only be explained by assuming a second source of heat in the sample. However, the initial excess of power (60 microwatts, or 0.08 per cent of the total) was about the same as the excess released by a 10-curie alpha source in a bottle filled with air. The tritium salt sample was sealed in a container having about the same relative amount of air.

Table 1

TRITIUM HALF-LIFE RESULTS

Calorimeter	Time Span from Jun. 5, 1959 (days)	Initial Power (watts)	Probable Error per Observation (microwatts)	Half-life (yrs)	Internal Probable Error (yrs)
39[a]	553-1456	-	-	12.361[b]	-
39	166-1456	0.072455	7.4	12.3572	0.0037
39	34-1456	0.072468	8.3	12.3449	0.0033
39	0-1456	0.072479	10.2	12.3346	0.0036
39	166-979	0.072460	7.4	12.3516	0.0091
51	35-1293	0.072474	20.0	12.3452	0.0084
77	Dec. 26, 1961 to Sept. 6, 1962	3.10233	675	12.194	0.028
Half-life from two grand-mean measurements (Aug. 23, 1959 to Apr. 13, 1962)				12.373	0.013

[a]The first six rows are measurements on a salt sample. Rows 7 and 8 are for a gas sample.

[b]Estimated.

Row 5 gives the results reported previously. Row 6 was obtained from Calorimeter 51 data (12.345 years). The agreement with Calorimeter 39 over the same time span is excellent. The initial power of the sample agrees within 0.01 per cent of the Calorimeter 39 value which is typical of previous comparisons.

Further half-life measurements have been made on the gaseous sample, and the results are presented in Rows 7 and 8 of Table 1. A slow variation caused the low half-life in Row 7 (12.194 years). In fact, these measurements were taken primarily to study slow variations.

The half-life in Row 8 (12.373 years) is essentially the same as the value of 12.372 years reported previously for the half-life of the gas sample. Both values were obtained from two grand-mean power measurements that were corrected by comparison to standard samples of polonium-210. The present value, however, was calculated with much more data included in the latter grand mean.

A most probable half-life and absolute probable error of 12.355 ± 0.010 years has been assigned to tritium from an inspection of Table 1 with the two lowest values eliminated for reasons cited above. Table 2 shows how this value compares favorably with the published results of other experimenters. The agreement between investigators is unusually good for half-life determinations. The limits on Jones' second value represent his internal precision, and it is difficult to judge the reliability of the value.

Table 2

TRITIUM HALF-LIFE BY VARIOUS INVESTIGATORS

Observer	Half-life (yrs)	Method
Mound Laboratory	12.355 ± 0.010	Calorimeter
Jones[a]	12.41 $^{+0.15}_{-0.25}$	Absolute counting
Jones[b]	12.262 ± 0.004	Helium-3 growth
Jenks, Ghormley, and Sweeton[c]	12.46 ± 0.1	Steady-state diffusion of helium-3 from a thin quartz capsule containing tritium oxide
Novick[d]	12.1 ± 0.5	Helium-3 growth

[a] *Phys. Rev.*, **72**, 972 (1947).

[b] *Phys. Rev.*, **75**, 701 (1949).

[c] *Phys. Rev.*, **83**, 537 (1951).

[d] *Phys. Rev.*, **100**, 124 (1955).

Half-life measurements will be continued with Calorimeters 39 and 77, but discontinued in Calorimeter 51 because of its poor precision during the last year. Measurements have been initiated on the salt sample with Calorimeter 90, which has an automatic loading system that is hermetically sealed from the room.[1] This method of operation may eliminate the slow variations. Fourteen assays over a span of 18 days gave a probable error per observation of only 3.0 microwatts, which is 2.5 times smaller than for Calorimeter 39 (Row 2, Table 1). The average power was only 0.005 per cent lower than for Calorimeter 39. The difference is so slight that the measurements from both calorimeters can be combined into a single half-life calculation.

[1] MLM-1144.

Polonium-208 and Polonium-209 in Irradiated Bismuth The yields of polonium-208 and polonium-209 from irradiation of multicurie quantities of polonium-210 in the Materials Test Reactor (MTR) have been calculated. The growth of polonium-208 or polonium-209 (if neutron capture of polonium-208 or polonium-209 is neglected) by (n, xn) reactions on polonium-210 is:

$$N_2 = \frac{N_1^0 \Phi \sigma_1 (e^{-\lambda_2 t} - e^{-\Lambda_1 t})}{\Lambda_1 - \lambda_2} \quad (1)$$

where N_2 = the number of atoms of polonium-208 or polonium-209

N_1^0 = the initial number of atoms of polonium-210 placed in the reactor

Φ = the thermal neutron flux

σ_1 = the effective cross section for the (n, xn) reaction of interest

Λ_1 = a modified decay constant for polonium-210

λ_2 = the decay constant of polonium-208 or polonium-209

The modified decay constant Λ_1 is required since polonium-210 is removed by radioactive decay as well as neutron capture. The value of Λ_1 is $(\lambda_1+\Phi\sigma_1)$, where λ_1 is the decay constant of polonium-210. For the calculations it was assumed that 100 curies (22.3 mg) of polonium-210 would be irradiated. The half-life of polonium-208 was taken to be 1055 days. Two separate calculations were made for the growth of polonium-209. In one case, a half-life of 103 years was used and in the second case, 16 years. The MTR flux was taken to be 8.8×10^{13} neutrons/(sec)(cm^2). The effective cross sections for $(n,2n)$ and $(n,3n)$ reactions on polonium-210 were taken to be 0.8 barn and 0.4 barn, respectively. The effective cross sections are used only because they give the observed reaction rate in the MTR neutron spectrum when multiplied by the thermal neutron flux. The values of the effective cross sections were calculated from the yields of polonium-208 and polonium-209 in MTR-irradiated bismuth.

Inspection of equation (1) shows that the growth of polonium-208 or polonium-209 is the product of a constant, $(N_1^0\Phi\sigma_1)/(\Lambda_1-\lambda_2)$, and a saturation term $(e^{-\lambda_2 t} - e^{-\Lambda_1 t})$. The saturation term is mainly a function of polonium-210 decay, and the $(e^{-\lambda_2 t})$ term can be taken as equal to 1.00 in the calculation of the polonium-209 yield because of the long half-life of polonium-209.

The values of the constant term in equation (1) for polonium-208 and polonium-209 are given in Table 3 with the weight of material and the activity that these values represent. The fraction of these quantities present as a function of time are shown in Figures 1 and 2. The results given in Table 3 and the growth curves of Figures 1 and 2 show that the production of small amounts of polonium-208 and polonium-209 is possible. However, it should be noted that large quantities of polonium-210 (relative to polonium-208 or polonium-209) would be present for a number of years in the irradiated material. The time at which the maximum amount of polonium-208 occurs is obtained by setting the first derivative of equation (1), with respect to time, equal to zero. The maximum polonium-208 content occurs at 466 days as noted on Figure 2.

Table 3

THE VALUE OF $(N_1^0\Phi\sigma_1)/(\Lambda_1-\lambda_2)$ FOR POLONIUM-208 AND POLONIUM-209

(n,xn) Product	$(N_1^0\Phi\sigma_1)/(\Lambda_1-\lambda_2)$ (atoms)	Weight (μg)	Activity (mC)
Po^{208}	3.88×10^{16}	13.4	7.93
Po^{209} ($t_{1/2}$ = 103 years)	7.16×10^{16}	26.9	0.447
Po^{209} ($t_{1/2}$ = 16 years)	7.76×10^{16}	26.9	2.88

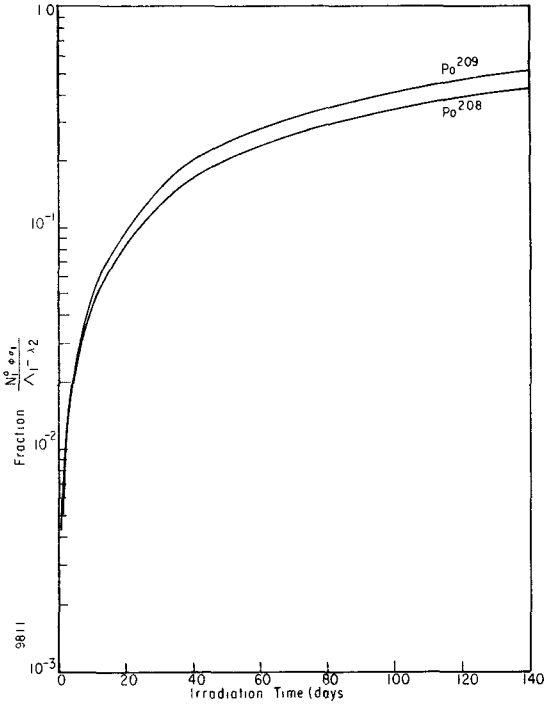

Figure 1. *The Growth of Polonium-208 and Polonium-209 as a Function of Irradiation Time.*

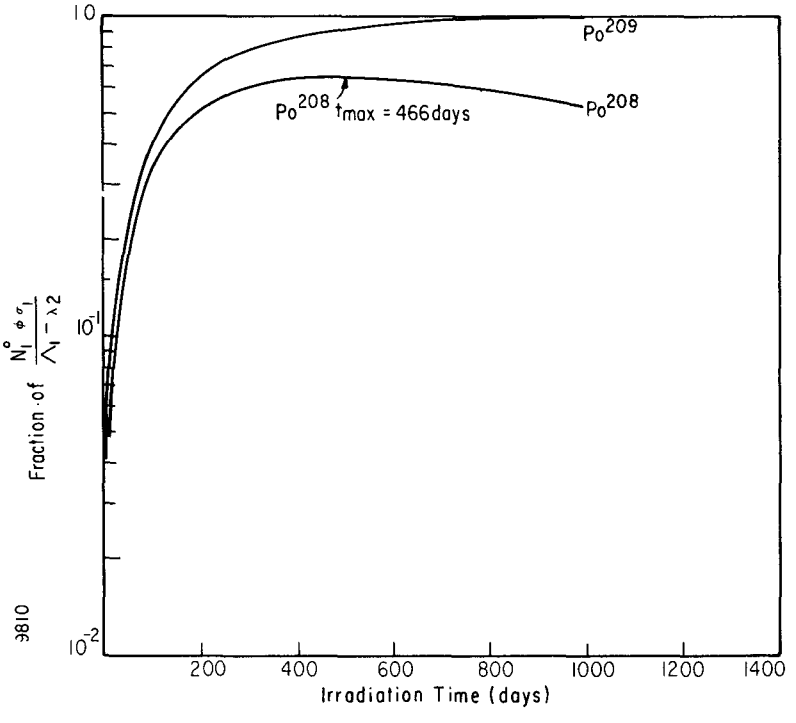

Figure 2. *The Growth of Polonium-208 and Polonium-209 as a Function of Irradiation Time.*

An accurate value for the polonium-208/polonium-209 alpha counting ratio in the polonium-208 from Argonne National Laboratory has been obtained. The ratio was determined from alpha pulse height analysis data by running the pulse amplifier at high gain. A good separation of the alpha particle groups of polonium-208 and polonium-209 resulted, as shown in Figure 3. The area under the two peaks was integrated by adding the actual number of counts in each channel in the peak. The present alpha activity ratio, polonium-208/polonium-209, is 18.89 ± 0.43. This value will be used in the calculation of the half-life of polonium-209 when the mass ratio of the two isotopes has been determined by mass spectroscopy.

Several long-term counting experiments have been initiated to obtain the half-lives of polonium-208 and polonium-209. Several samples of different isotopic mixtures of polonium-208, polonium-209, and polonium-210 have been accumulated during the work on polonium-208 and polonium-209. By comparing the counting rates of the three alpha particle groups of the respective isotopes as a function of time, it should be possible to determine the half-lives of polonium-208 and polonium-209; polonium-210, for which the half-life is known, will be used as an internal standard.

Decay Scheme Studies Several theoretical treatments of the nuclear energy levels around neutron number 126 and proton number 82 have been reported in the literature. The level scheme for $^{125}_{83}Bi^{208}$ is complicated by the fact that the nucleus contains one proton beyond a closed shell and one less neutron than a closed shell. Mixing calculations of the nuclear configurations for one particle and one hole is difficult.

Calculations by Wahlborn[1] and by Huang Wei-Chin[2] indicated a low-lying level from 0.06 to 0.09 Mev above the ground state of bismuth-208. This low-lying level could explain the complex gamma-ray decay at about 0.600 Mev seen in the electron capture decay of polonium-208, in coincidence with a gamma ray of 0.30 Mev. A level scheme constructed from the present experimental data is shown in Figure 4.

Huang Wei-Chin also indicated levels at 1.41 and 1.47 Mev above the ground state of bismuth-208. Thus, the energy available for the electron capture decay (Q_{EC}) of polonium-208 is of interest. The Q_{EC} has been estimated to be 1.31 Mev.[3] This value can also be calculated from semi-empirical mass equations. Cameron's masses lead to a value of 1.73 Mev;[4] the Koenig, Mattauch, and Wapstra data give 1.43 Mev.[5] Q_{EC} may also be estimated by the closed-cycle method; but again, experimental data for such a calculation using the Pb^{204}-Po^{208}-Bi^{208}-Tl^{204} closed cycle is incomplete. The alpha decay energy of bismuth-208 is not known experimentally. Experiments are in progress to determine whether levels at about 1.4 Mev in bismuth-208 are populated in the electron capture decay of polonium-208.

Determination of Coincidence Correction

It was shown earlier that a small absolute error in a "known" half-life value can produce a relatively large error in the value computed for the resolution time;[6] and conversely, that an error in the resolution time used to determine a half-life can result in a significant absolute error in the reported half-life. Furthermore, the use of unweighted counting data, which has the effect of overweighting the relatively unreliable lower end of the decay curve produces inaccurate and imprecise results. These effects are shown graphically in Figures 5 and 6. The alpha counting rate of an equilibrium mixture of lead-211 and bismuth-211 was determined at two-minute intervals over a period of more than four hours in the chamber of a gas flow proportional counter. The data were analyzed by the method of least squares for several assumed values of τ, the resolution time, and for several assumed values of $T_{1/2}$, the half-life.

---

[1]Wahlborn, *Nuclear Phys.*, **3**, 644 (1957).

[2]Huang Wei-Chin et al., *Acta Phys. Sinica*, **16**, 13 (1960)

[3]Strominger, Hollander, and Seaborg, *Revs. Modern Phys.*, **30**, 585 (1958).

[4]Cameron, "A Revised Semi-empirical Atomic Mass Formula," Chalk River Report, CRP-690, March, 1957.

[5]Koenig, Mattauch, and Wapstra, *Nuclear Phys.*, **31**, 18 (1962).

[6]MLM-1151.

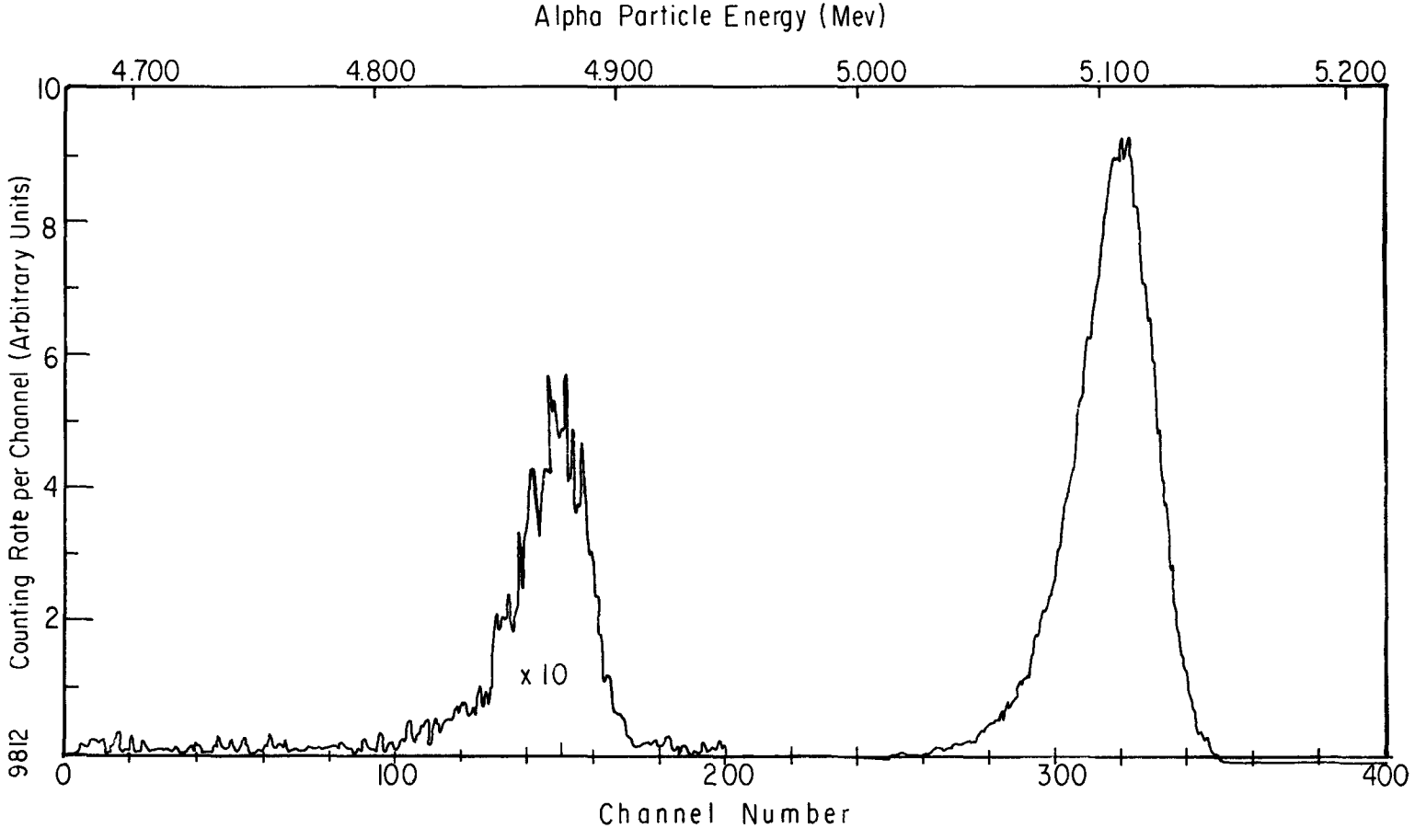

Figure 3. *Alpha Spectrum of Polonium in Argonne Polonium-208.*

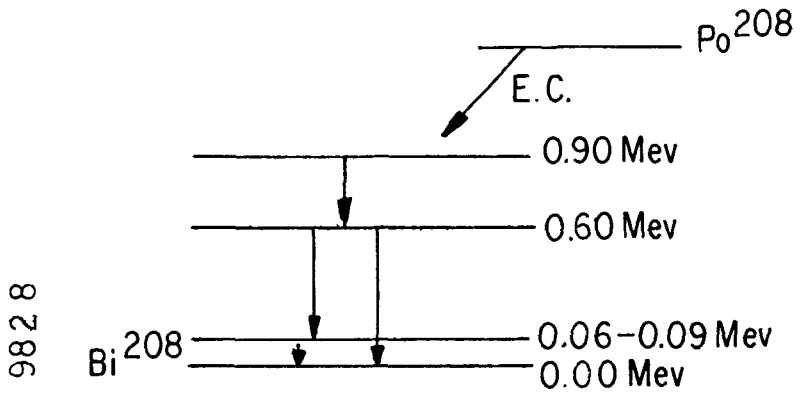

Figure 4. *Tentative Decay Scheme for Polonium-208.*

The same data were used for computing the curves in Figures 5 and 6; however, in Figure 5 the data were unweighted, while in Figure 6 the data were weighted inversely as the squares of their probable errors. Each set of computations yielded two parabolas and two intersecting straight lines. The straight lines show the variation of $T_{1/2}$ with different assumed values of τ, and the variation of τ with different assumed values of $T_{1/2}$. The parabolas show the variation in the sum of the squares of the deviations for different values of either $T_{1/2}$ or τ. The vertex of each parabola is indicated by a pair of dotted lines representing the smallest sum of the squares on the deviations and the corresponding "best" value of either $T_{1/2}$ or τ.

It is especially noteworthy that the two straight lines of Figure 5 have significantly different slopes while the corresponding lines of Figure 6 are nearly congruent. In addition, the intersection of the two straight lines of Figure 5 occurs at a point significantly different from the intersection of the axes of the two parabolas. In Figure 6 both pairs of lines intersect at nearly the same point.

Since for any assumed value of either $T_{1/2}$ or τ there should be a unique solution for the other variable, it seems reasonable to expect that a single straight line should represent the variation of $T_{1/2}$ with τ regardless of which is selected as the independent variable. That is, if all assumptions are correct, the intersecting lines should be congruent and should coincide with the intersection of the axes of the parabolas. This condition is approximated more closely in Figure 6, representing weighted data, than in Figure 5, representing unweighted data.

The use of Chauvenet's criterion for the rejection of inconsistent data can often be useful in eliminating inconsistent data which unduly influence the calculations. However, if the data are consistent, no significant improvement results from the use of rejection criteria. As shown in Table 4, the use of Chauvenet's criterion does not greatly improve the agreement of the results obtained with weighted data.

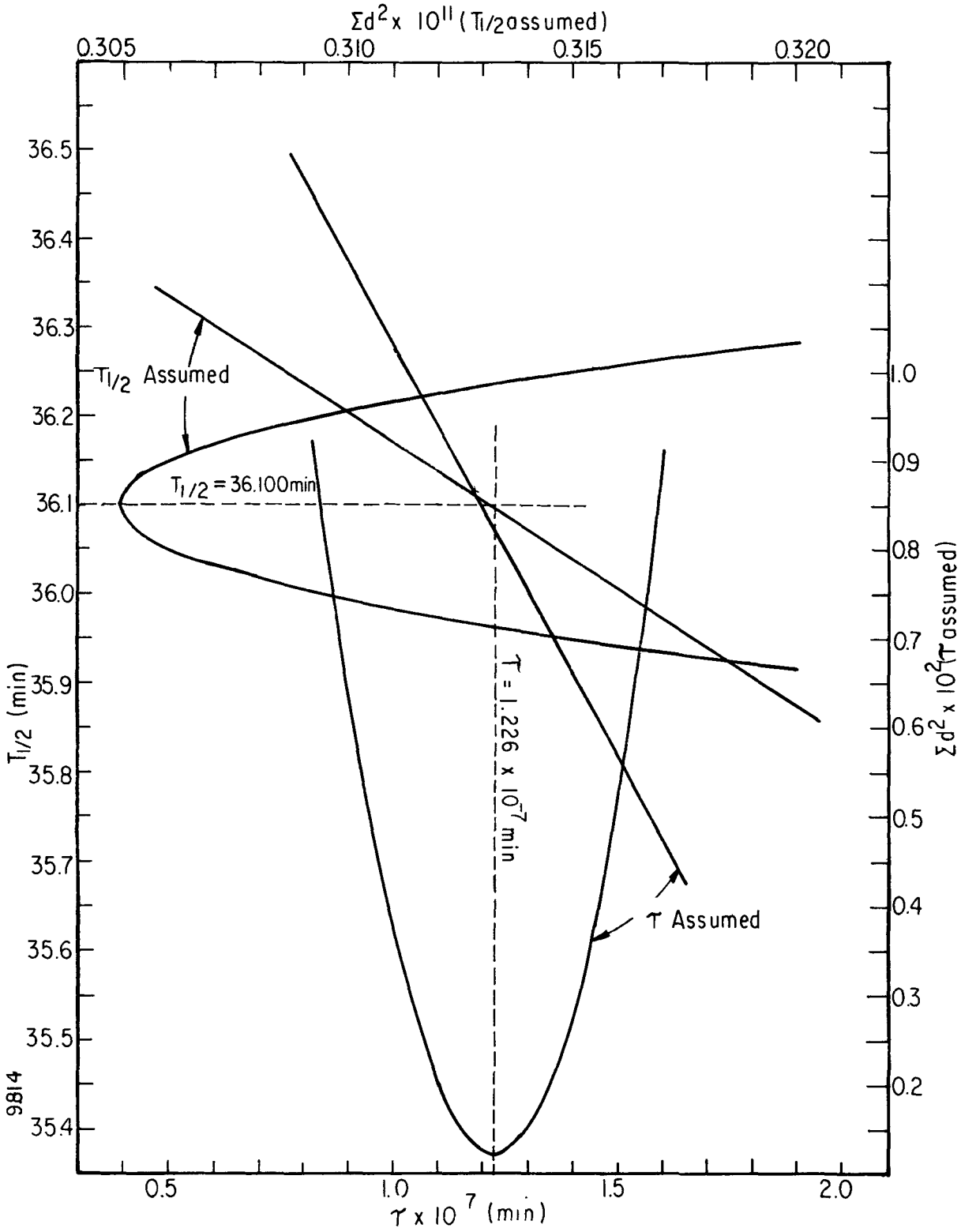

Figure 5. *Variation of the Functions $\tau = f(x)$ and $T_{1/2} = f(\tau)$ with Unweighted Data.*

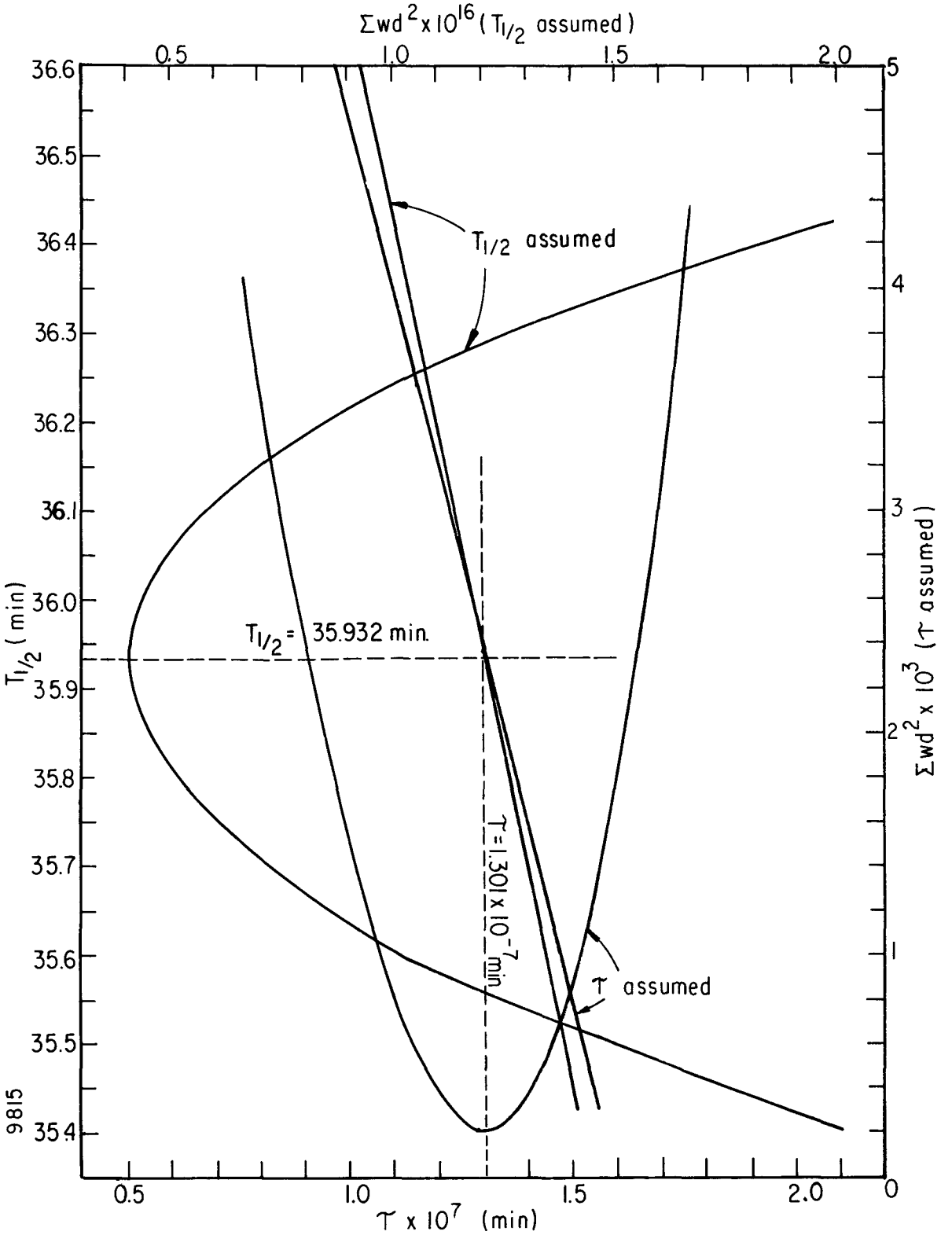

Figure 6. *Variation of the Functions $\tau = f(T_{1/2})$ and $T_{1/2} = f(\tau)$ with Weighted Data.*

Table 4

HALF-LIFE OF LEAD-211 AND RESOLUTION TIME OF A PROPORTIONAL COUNTER[a]

Readings Weighted	Chauvenet's Criterion Applied	Maximum Count Rate (cpm)	Half-life (min.)	Resolution Time (min x 10^7)
No	No	1.4×10^6	36.075 ± 0.007	(1.226 ± 0.001)
			(36.100 ± 0.062)	1.212 ± 0.172
Yes	No	1.4×10^6	35.941 ± 0.008	(1.301 ± 0.001)
			(35.932 ± 0.019)	1.305 ± 0.004
Yes	Yes	1.4×10^6	36.013 ± 0.007	(1.250 ± 0.001)
			$(36.000 \pm 0.016$	1.269 ± 0.003
Yes	No	1.0×10^6	36.075 ± 0.007	(1.187 ± 0.002)
			(36.068 ± 0.017)	1.191 ± 0.005
Yes	No	0.5×10^6	36.139 ± 0.013	(1.087 ± 0.003)
			(36.121 ± 0.031)	1.112 ± 0.019

[a]By Jordan's variational method. Parentheses indicate the "best" value of the quantity varied.

Table 4 also shows the change in computed half-life and resolution time which results from eliminating data above certain counting rate levels. This effect is shown in more detail in Table 5, where the half-life and resolution time are computed for various segments of the decay curve.

Since it is axiomatic that the half-life of a radioisotope is perfectly constant, any trend in the computed half-life, as indicated in Table 5, must be attributed to a trend in the resolution time of the counter. The computed half-life values of Table 5 are plotted in Figure 7 as a function of the maximum counting rate used in the calculations. It is seen that there is a continuous trend towards lower values of the computed half-life as the upper counting rate limit increases. At the lower counting rates, the computed half-life values approach a constant value of approximately 36.15 minutes.

The weighted mean of the six half-life values obtained with upper counting rate limits of less than 10^6 counts per minute (data numbered 16 and higher) is 36.102 ± 0.015 minutes. However, the individual half-life values are not randomly distributed around the mean; the three highest segments of the decay curve yield values below the mean, while the three lowest segments yield values above the mean.

It must be tentatively concluded that the "known" half-life method for determining the resolution time of a counting instrument can yield only an average value for the counting range used in the computations. Conversely, the absolute accuracy of any reported half-life value is doubtful if that value was computed from counting data to which a single resolution time was applied over the entire counting range.

Although high precision can be obtained by the use of counting data covering many half-lives (e.g., the results for the data numbered 1-82 in Table 5), it would be preferable, from the standpoint of absolute accuracy, to make a series of relatively imprecise computations, with data covering only a short segment of the decay curve, possibly no greater than a single half-life. This hypothesis is now being tested, and the computed half-life results should be available in the near future.

Table 5

HALF-LIFE OF LEAD-211 AND RESOLUTION TIME OF A PROPORTIONAL COUNTER AS FUNCTIONS OF THE COUNTING RATE LEVEL[a]

Data Identification Numbers	Count Rate Limit (cpm x 10^{-4}) Upper	Lower	Half-life (min)	Resolution Time (min x 10^{7})
1-82	140.4	1.1	35.941 ± 0.008 (35.932 ± 0.019)	1.305 ± 0.004 (1.301 ± 0.001)
1-42	140.4	26.9	35.572 ± 0.013 (35.548 ± 0.060)	1.423 ± 0.004 (1.415 ± 0.001)
6-47	119.9	16.3	35.828 ± 0.011 (35.812 ± 0.044)	1.318 ± 0.004 (1.312 ± 0.001)
11-52	100.0	13.5	35.947 ± 0.011 (35.932 ± 0.044)	1.258 ± 0.005 (1.251 ± 0.002)
16-57	84.4	11.2	36.088 ± 0.012 (36.069 ± 0.044)	1.178 ± 0.007 (1.166 ± 0.003)
21-62	70.9	9.2	36.041 ± 0.013 (36.017 ± 0.051)	1.213 ± 0.010 (1.194 ± 0.004)
26-67	59.3	3.8	36.062 ± 0.014 (36.036 ± 0.046)	1.224 ± 0.014 (1.200 ± 0.003)
31-72	46.0	1.6	36.133 ± 0.016 (36.103 ± 0.047)	1.132 ± 0.021 (1.094 ± 0.006)
36-77	38.5	1.3	36.200 ± 0.016 (36.175 ± 0.043)	0.967 ± 0.029 (0.928 ± 0.007)
41-82	28.1	1.1	36.151 ± 0.018 (36.123 ± 0.043)	1.116 ± 0.043 (1.092 ± 0.010)

[a]By Jordan's variational method. Parentheses indicate the "best" value of the quantity varied.

An alternative to the use of a short segment of the decay curve is provided by the decaying pair method of half-life determination, which has been successfully applied to the half-life of radium-223.[7] The decaying pair method eliminates the need for a knowledge of the resolution time of a proportional counter, but assumes that the resolution time is a constant and that there exists a constant ratio between the true disintegration rates of any two samples of the same radioisotope. If the two disintegration rates do not differ greatly in magnitude, the assumption that the resolution time is a constant should be valid.

For purposes of computation it is not necessary to have two different samples. Data recorded at a fixed time interval apart can be treated as having been produced from two separate sources of different magnitude. Thus, of the 82 individual observations used in the computations for Tables 4 and 5, there were 69 pairs of data which could be treated as originating from two samples, the ratio of whose magnitudes corresponded exactly to two minutes' decay of lead-211. Similarly, a 10-minute time interval yielded 46 pairs, a 20-minute interval 30 pairs, and so on.

[7]MLM-1148.

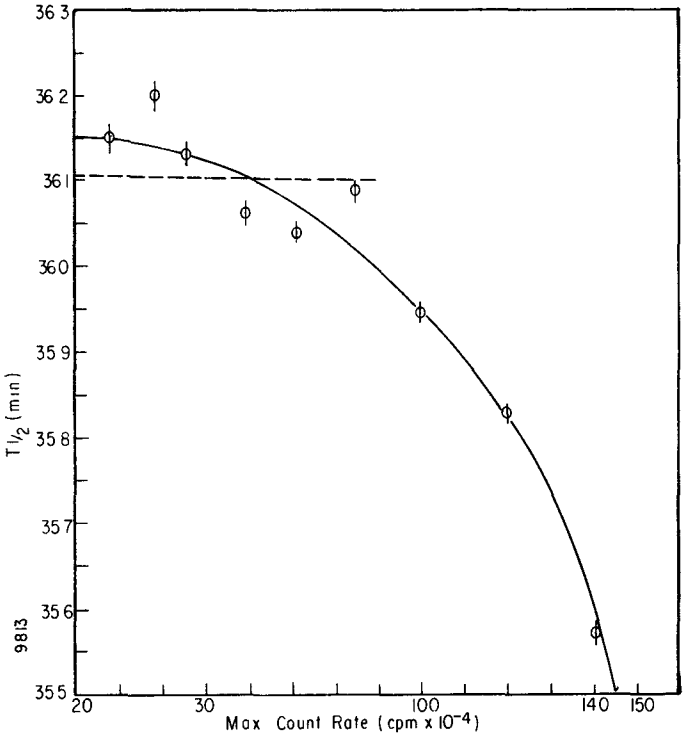

Figure 7. *Variation of Calculated $T_{1/2}$ with Maximum Counting Rate.*

The results of a trial run with unweighted data are given in Table 6. Only those time intervals yielding 20 or more pairs are reported in the tabulation. The weighted average of the 35 half-life values is 36.043 ± 0.030 minutes; there does not appear to be any significant trend. It is expected that the results for weighted data will be available next month.

Table 6

HALF-LIFE OF LEAD-211 BY DECAYING PAIRS (UNWEIGHTED DATA)

Time Interval (min)	Number of Pairs	Half-life (min)	Time Interval (min)	Number of Pairs	Half-life (min)
2	69	36.168 ± 0.273	35	24	35.871 ± 0.022
4	61	36.121 ± 0.161	37	24	35.909 ± 0.026
6	56	36.118 ± 0.093	39	26	36.103 ± 0.035
8	51	36.044 ± 0.087	41	29	36.020 ± 0.025
10	46	36.051 ± 0.071	43	32	36.013 ± 0.023
12	41	36.017 ± 0.047	45	31	36.090 ± 0.032
14	38	35.941 ± 0.047	47	31	36.048 ± 0.028
16	34	36.057 ± 0.044	49	31	36.117 ± 0.025
18	33	36.117 ± 0.041	51	31	36.149 ± 0.024
20	30	36.103 ± 0.041	53	31	36.085 ± 0.025
22	25	36.139 ± 0.031	55	30	36 059 ± 0.026
23	20	35.787 ± 0.056	57	29	36.050 ± 0.021
24	21	36.096 ± 0.032	59	28	36.074 ± 0.020
25	22	35.760 ± 0.049	61	26	36.117 ± 0.020
27	21	35.826 ± 0.049	63	24	36.098 ± 0.017
29	22	35.793 ± 0.046	65	24	36.077 ± 0.020
31	22	35.821 ± 0.036	67	21	36.063 ± 0.023
33	23	35.955 ± 0.035			

Uranium-234 Separation

Milligram quantities of uranium-234 are being separated from aged plutonium-238 solutions by ion exchange and solvent extraction techniques. The uranium is separated from the bulk of the plutonium in solution by an anion exchange resin. Plutonium and other impurity elements are further removed from the uranium by a hexone extraction. Finally, a thenoyltrifluoroacetone (TTA) extraction removes the last traces of plutonium from the uranium. One batch of feed solution (B63) was processed and yielded 14 milligrams of uranium-234. A second batch (5H) is being processed, but analytical data are not yet available.

An 825-milliliter volume of 5H feed solution containing about 22 grams of plutonium was processed through the ion exchange step in six separate runs. Processing details and analytical results of the runs will be reported when the processing of the entire feed solution is complete. In most runs the ferrous sulfamate or hydroxylamine reduction procedures, which were described previously, resulted in ion exchange raffinates containing about 0.1 per cent of the starting plutonium, a satisfactory decontamination level.

A 44-inch pulse-type solvent extraction column was assembled to investigate the feasibility of a continuous solvent extraction process for separating uranium-234 from solution. The column consisted of a 30-inch length of one-inch insdie diameter Pyrex glass pipe with four-inch diameter disengaging chambers located at the top and bottom of the pipe. The ends were closed off with ¼-inch thick stainless steel plates with feed and and exit lines welded through the plates. Thirty stainless steel sieve plates, one inch in diameter and containing 23 per cent free area, were strung on a ⅛-inch stainless steel rod with one-inch lengths of stainless steel tubing as spacers. Micro-bellows pumps were used to pulse the column and circulate the feed solutions. Flow rates and operating parameters of the column are presently being determined.

Potassium Plutonium Sulfate Dihydrate

Inorganic Chemistry of Potassium Plutonium Sulfate Dihydrate The thermogravimetric studies of $K_4Pu(SO_4)_4 \cdot 2H_20$ and $Pu(SO_4)_2 \cdot 4H_20$ are complete. A final series of experiments verified the thermograms which were reported previously. Differential thermal analysis of $K_4Pu(SO_4)_4 \cdot 2H_20$ is also complete A final series of experiments showed that the DTA thermogram previously reported for $K_4Pu(SO_4)_4 \cdot 2H_2O$ is essentially correct. Final DTA thermograms for $Pu(SO_4)_2 \cdot 4H_20$ and a mixture of $2K_2SO_4 + Pu(SO_4)_2 \cdot 4H_2O$ are now being studied. Samples of $K_4Pu(SO_4)_4 \cdot 2H_2O$ and $Pu(SO_4)_2 \cdot H_2O$ were submitted for x-ray diffraction pattern studies. The salts were sampled just prior to, and immediately following, composition or phase changes as predicted by the DTA and TGA thermograms. Data from the x-ray studies are not yet available.

The study of the solubility of $K_4Pu(SO_4)_4 \cdot 2H_2O$ as a function of the sulfate ion concentration was previously reported. The solubility of the compound as a function of the hydrogen ion concentration was determined. The solubility of the complex salt is constant between 0.1 molar and two molar hydrogen ion concentration. Previously, the solubility of the compound was predicted to be acid dependent. This theory was based on a mechanism of formation such as:

$$Pu^{+4} + n\ HSO_4^- \rightleftharpoons Pu(SO_4)_n^{+4-2n} + n\ H^+$$

where n (or$_n$) = 1, 2, 3, 4. However, a mechanism such as:

$$Pu^{+4} + n\ HSO_4^- \rightleftharpoons H_nPu(SO_4)_n^{+4-2n}$$

may not be acid dependent. This mechanism indicates the existence of the complex acid $H_4Pu(SO_4)_4$.

Solubility Study Potassium plutonium sulfate dihydrate is being evaluated as a calorimetric standard. The solubility of $K_4Pu(SO_4)_4 \cdot 2H_2O$ was found to vary with the potassium concentration of the solution. Test solutions were prepared with 0.959 molar sulfuric acid and concentrations of potassium chloride varying from 0.1 to 0.5 molar. These solutions were saturated with $K_4Pu(SO_4)_4 \cdot 2H_2O$ and maintained at 25°C for seven days. Following this period, each solution was sampled, filtered, and analyzed. The results of this study are shown in Figure 8 where log [total Pu] is plotted against -log $[K^+]$. The slope of the line is 4.08. A slope of 4.00 was determined using the theoretical solubility product function:

$$\log Pu = \log K_{sp} + \log \alpha - \log [SO_4]^4 - 4 \log [K^+]$$

Further studies will be made of the $[H^+]$ and $[K^+]$ solubilities.

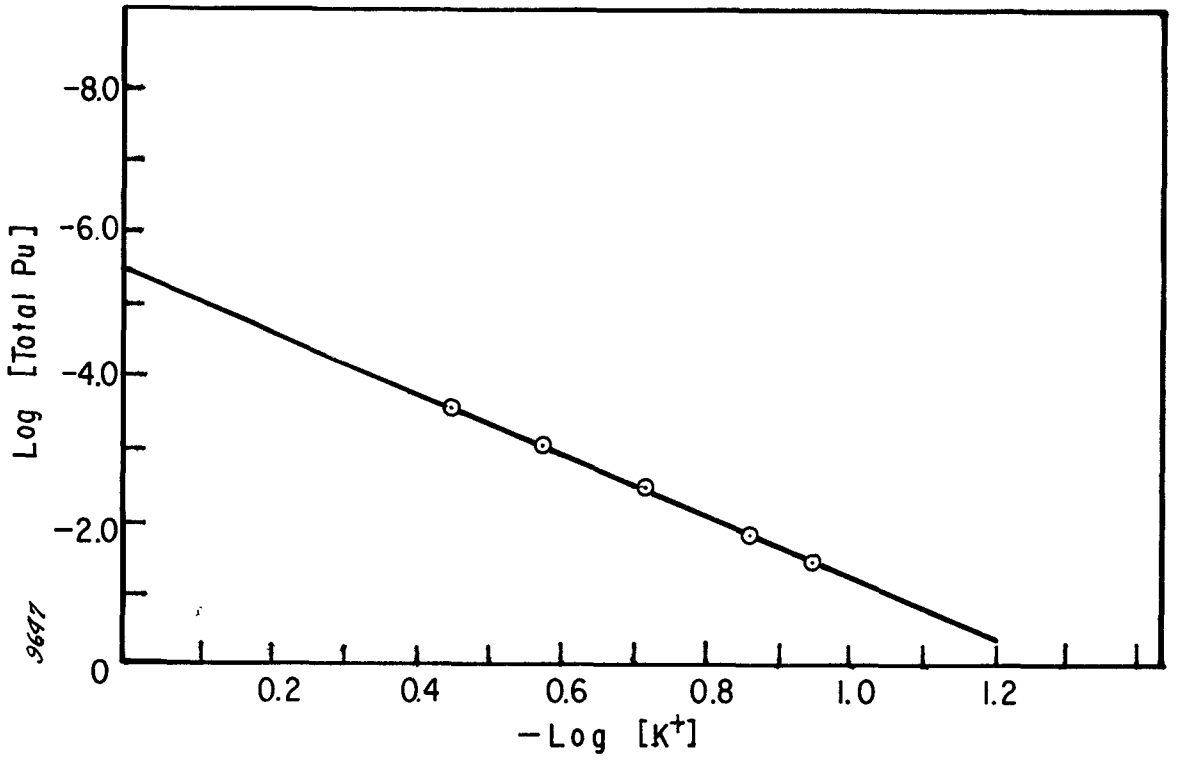

Figure 8. *$K_4Pu(SO_4)_4 \cdot 2H_2O$ Solubility.*

Thermal Analysis of $K_4Pu(SO_4)_4 \cdot 2H_2O$ Studies are being made on the thermal behavior of potassium plutonium sulfate dihydrate, $K_4Pu(SO_4)_4 \cdot 2H_2O$. Thermogravimetric analysis (TGA) results, shown in Figure 9, indicate that the compound loses two moles of water when heated to 150°C. This reaction corresponds, in Figure 10, either to point *A* or to points *A* and *B*. The temperatures shown in Figure 9 are equilibrium temperatures and are, therefore, only roughly compariable to the temperatures shown in the thermograms.

After potassium plutonium sulfate dihydrate was heated at 155°C for four hours, the thermogram shown in Figure 11 was obtained by differential thermal analysis (DTA). Thus, point *B* common to the curves in both Figures 10 and 11, does not represent loss of water from the compound. This temperature inflection must represent a structural transformation in the crystal.

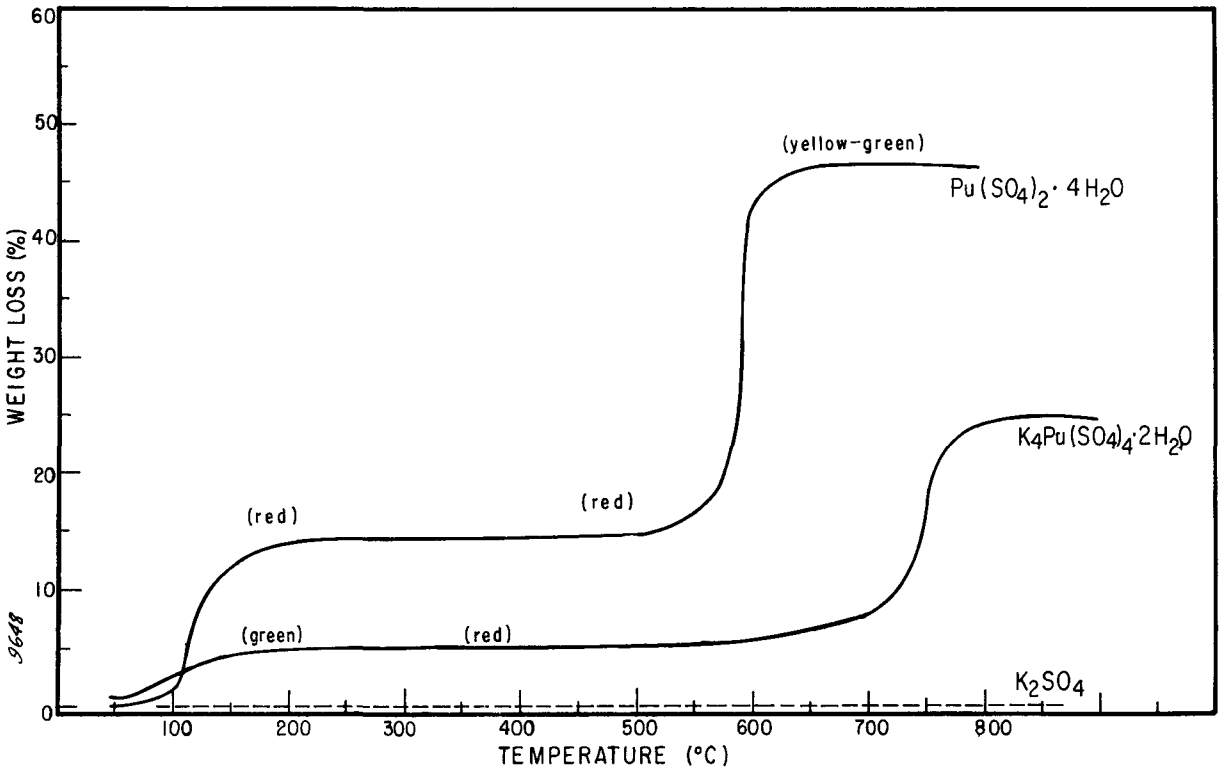

Figure 9. *Thermogravimetric Analysis of Potassium Plutonium Sulfate Dihydrate, Plutonium Sulfate Tetrahydrate, and Potassium Sulfate.*

The DTA thermograms of plutonium sulfate tetrahydrate shown in Figures 12 and 13 indicate that a similar phenomenon takes place when four moles of water are removed from the compound. Curve *A* (Figure 13) was eliminated by heating the tetrahydrate at 150°C for four hours, but curve *B* remained. Therefore, a crystal rearrangement must also take place in plutonium sulfate immediately after the loss of four moles of water. Figure 14 shows the DTA thermogram of the alpha-to-beta phase transition which potassium sulfate undergoes with heating. This inflection should appear at point *D*, Figures 10 and 15, and 16, if free potassium sulfate were present in the sample. Figure 16 shows this transition on a portion of a mixture of one mole of plutonium sulfate and two moles of potassium sulfate. The alpha-to-beta phase transition of potassium sulfate is observed in the thermogram of the mixture to such an extent that point *E*, Figures 10 and 15, is not observed in Figure 16; point *D* is not observed in Figure 10. Therefore, either the compound potassium plutonium sulfate dihydrate is not thermally decomposed at point *C*, Figure 10; or, if decomposition does occur at point *C*, a solid solution results. Points *E* and *F* in Figures 10 and 15 represent the removal of two moles of SO_3 from the compound. This reaction is represented by points *C* and *D*, Figures 12 and 13, for plutonium sulfate.

X-ray powder diffraction patterns, obtained from samples taken after the ignition of potassium plutonium sulfate dihydrate to temperatures indicated by numbers 1 through 10, Figure 10, were inconclusive. The patterns showed many lines which were too diffused for quantitative treatment. The x-ray data indicate that a high degree of hydrogen bonding exists in samples 1 - 3. This bonding may be due to water bridging. That is, potassium plutonium sulfate dihydrate may precipitate as long-chained molecule. This reaction may account for the slow rate of formation of the precipitate. Samples 4 - 8 appeared to be amorphorus. Patterns from samples 6 and 7 were similar, indicating either that thermal decomposition did not occur at point *C*, in Figure 10, or that a solid solution results upon decomposition. Patterns from samples 9 and 10 showed the presence of a mixture of potassium sulfate and plutonium oxide. Sample 10 was shown to contain stoichiometric plutonium oxide which was a face-centered cubic in space group *Fm3m*; its lattice parameter was equal to 5.396 ± 0.001 angstroms.

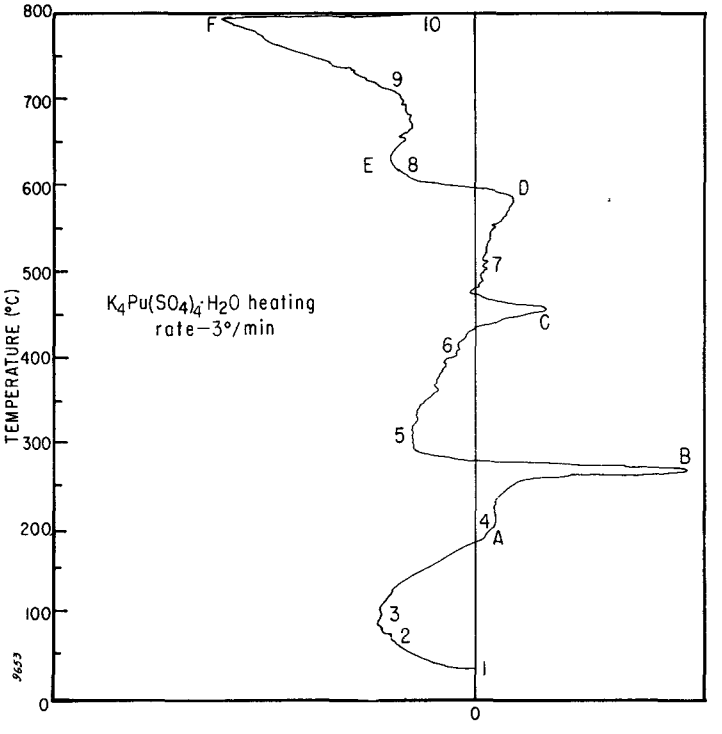

Figure 10. *Thermogram of Potassium Plutonium Sulfate Dihydrate.*

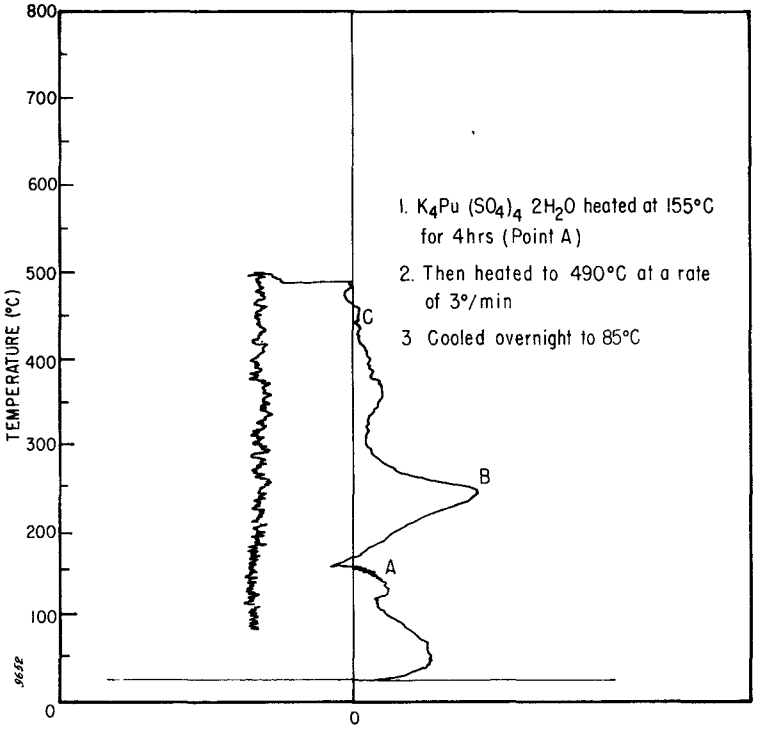

Figure 11. *Thermogram of Potassium Plutonium Sulfate Dihydrate.*

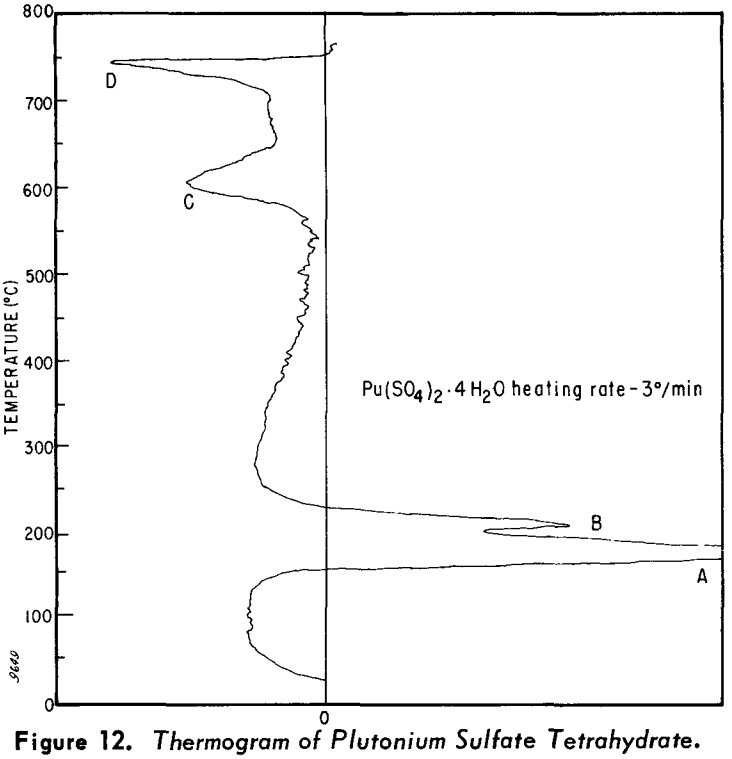

Figure 12. *Thermogram of Plutonium Sulfate Tetrahydrate.*

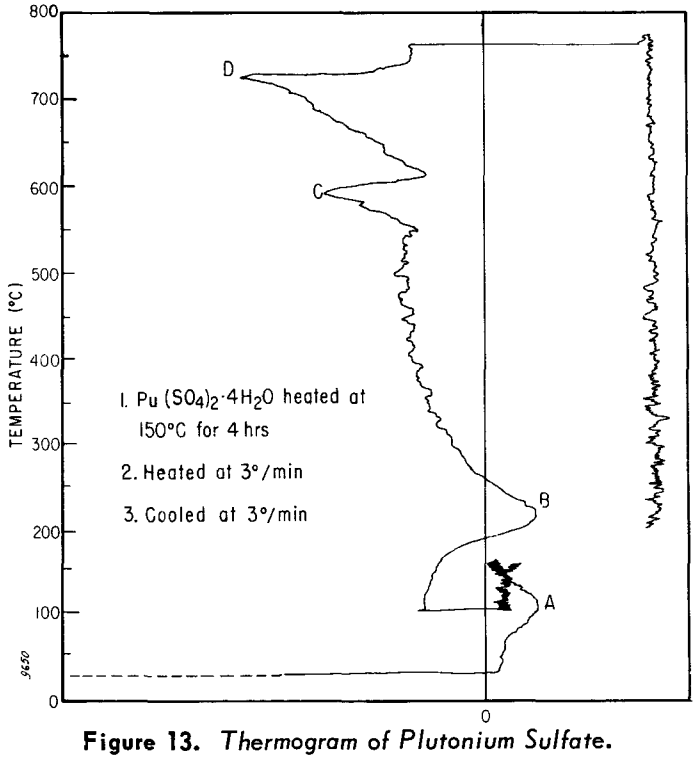

Figure 13. *Thermogram of Plutonium Sulfate.*

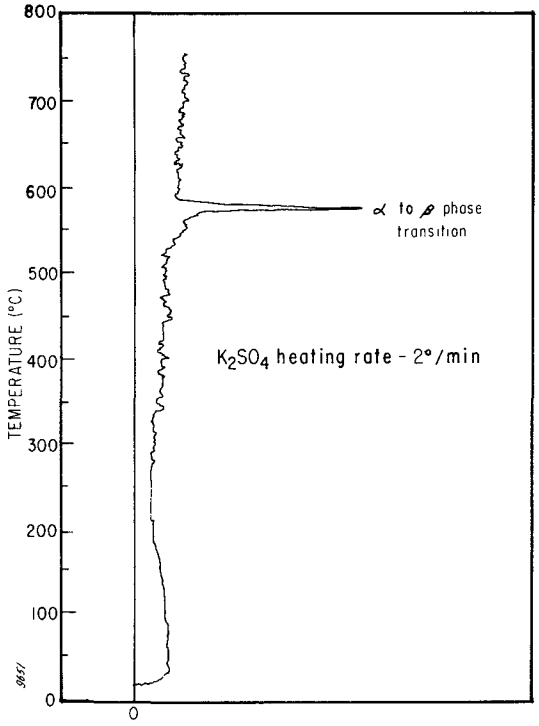

Figure 14. *Thermogram of Potassium Sulfate.*

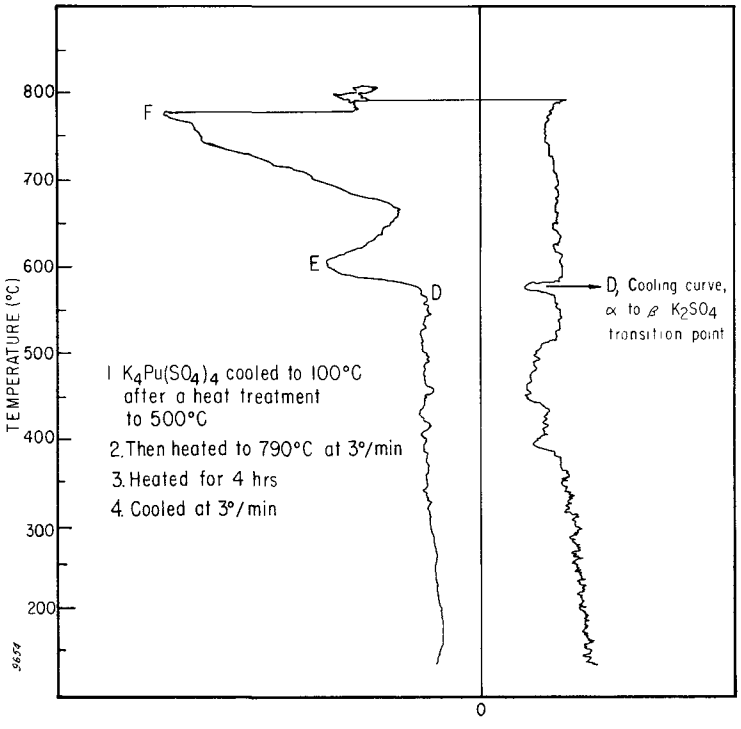

Figure 15. *Thermogram of Potassium Plutonium Sulfate.*

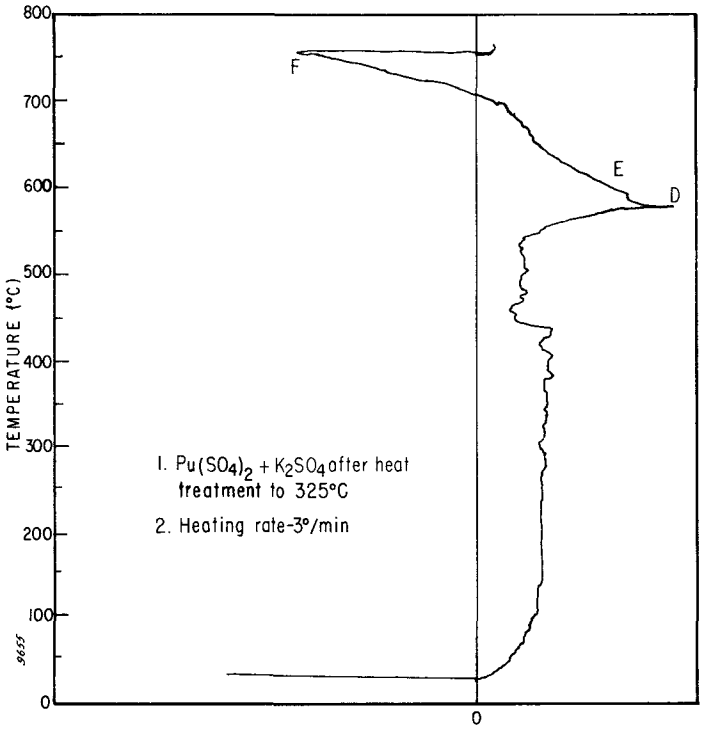

Figure 16. *Thermogram of Stoichiometric Mixture of Plutonium Sulfate and Potassium Sulfate.*

Processes are being developed for separating and purifying the isotopes of a number of elements including hydrogen, the noble gases, carbon, and uranium. Potential sources of supply of these materials are being evaluated.

Carbon-13

Methane Purification Two cascaded, 24-foot, hot-wire thermal diffusion columns are being used for the removal of heavy gaseous impurities, such as nitrogen, carbon monoxide and ethane from 99 per cent pure natural methane. A three-column series system is being used for carbon-13 enrichment of natural methane. The carbon-13 content is seven per cent in 89 per cent methane at the bottom of the third stage, and the flow rate is about four milliliters per hour.

A concentric-tube column was connected to a six-column, four-stage cascade unit for the partial separation of mass 17 methane. Gas is being fed through the stripping section of the cascade at a rate of 30 to 35 liters per day. Heavy impurities are being drawn off the bottom of the last stage. The middle of the fifth stage shows a concentration of 10 per cent carbon-13 in 98 per cent total methane. The transport of carbon-13 into the column system is less than expected for single column performance. The lack is probably due to flow restrictions, pressure excursions, and flow disturbances arising from non-smooth operation of one or more of the components of the feed, draw-off and circulating systems.

Measurements of Carbon Monoxide Transport Coefficients Experiments were begun to measure thermal diffusion column transport coefficients for the various carbon monoxide masses. Accurate values of the experimental hot wall temperature are required for comparison of results with theory. Optimum temperatures lie below the useful range of an optical pyrometer; therefore, hot-to-cold pressure ratios were used to establish the center-wire temperature. First, gas was admitted to the cold column to an arbitrary pressure; then the wire current was adjusted so that the pressure rose to a value calculated for an average temperature corresponding to the desired wire temperature.

Calculation of the average temperature was based on the fact that the total mass of gas in the column was the same before and after heating. Therefore, the gas density in the cold column was equal to the average density in the hot column:

$$\rho_2 = \frac{2}{r_2^2 - r_1^2}\int_{r_1}^{r_2} \rho r dr$$

where ρ is the density and r is the radial coordinate in the column. Subscripts 1 and 2 refer to the hot and cold walls, respectively. Since ρ is proportional to p/T, where p is the pressure and T is the absolute temperature, the pressure ratio before and after heating is as follows:

$$\frac{p_1}{p_2} = \frac{(r_2^2 - r_1^2)}{2T_2\int_{r_1}^{r_2}\left(\frac{r}{\overline{T}}\right)dr} = \frac{T}{T_2}$$

The required average temperature is then given by:

$$\overline{T} = \frac{r_2^2 - r_1^2}{2\int_{r_1}^{r_2}\left(\frac{r}{\overline{T}}\right)dr}$$

The evaluation of the integral requires the knowledge of r as a function of T. Application of a heat balance gives the temperature distribution in implicit form:

$$\ln \frac{r}{r_1} = \ln \frac{r_2}{r_1} \cdot \frac{\int_{T_1}^{T} \lambda dT}{\int_{T_1}^{T_2} \lambda dT}$$

where λ is the thermal conductivity of the gas. Numerical techniques must be used to obtain values of the average temperature from these two expressions.

The average temperature as a function of wire temperature has been calculated for carbon monoxide in a ¾-inch column with a $\frac{1}{16}$-inch hot wire. A cold wall temperature of 20°C was assumed. The results are listed in Table 7. Also given are average temperature values calculated from a simplified expression derived earlier.[8]

Table 7

AVERAGE TEMPERATURE AS A FUNCTION OF WIRE TEMPERATURE

Wire Temperature (°C)	Average Temperature (°C)	Average Temperature by Simplified Method (°C)
520	126	119
620	147	139
720	169	159
820	188	178

Chemical Exchange Two specific methods for the production of carbon-13 by chemical exchange are the cyanide method and the nonaqueous carbamate method.[9] The cyanide exchange method has been developed to a greater extent than the nonaqueous carbamate method; therefore, an experimental system for studying the nonaqueous carbamate system is presently being designed. The object of the experimental studies is to increase the separation, so the system must be large enough to yield a measurable separation of the isotopes. Secondly, the system must be versatile enough to allow a wide range of experiments. To insure a good separation in a reasonable time under varying operating conditions, the experimental column should be seven feet long and about one-half inch in diameter. The column should be vacuum jacketed to maintain various constant operating temperatures.

The column is refluxed by catching the liquid carbamate off the bottom of the column in a boiler maintained at or above 65°C. Carbon dioxide which boils off can be sampled and analyzed. The carbon dioxide feed point is situated above the product withdrawal point by either an S-tray containing liquid carbamate or a column extension through which liquid carbamate is flowing. Amine, which is regenerated in the boiler, is withdrawn through a connecting tube in the bottom of the boiler, cooled in a condenser, and pumped back to the top of the column where it reacts with the feed carbon dioxide.

[8] MLM-1146.

[9] MLM-1157.

The system is expected to yield a separation factor up to 1.39 depending upon the operating conditions. This value was calculated from the results obtained using monoethanolamine in a methanol solution at 35°C. The effect of various solvents and operating temperatures and pressures other than atmospheric will be investigated to increase the separation.

This system was compared with the cyanide method on a production scale. An extension of the carbamate system was calculated for a number of columns in cascade. The results of the calculations made for an eight-stage cascade (column diameters from 1.4 inches to 0.5 inch) with each stage capable of a 1.39 separation factor, show that about 0.4 gram of carbon-13 per day at 12 per cent concentration could be obtained. Becker's cyanide plant for the production of carbon-13 was typical: it consisted of a four-stage cascade (column diameters from 1.5 inches to 0.5 inch) totalling about 35 feet; the yield was about 0.25 gram of carbon-13 per day at almost 12 per cent concentration.[10]

It appears that the carbamate method is competitive with the cyanide method if no problems in the extension of the carbamate system are encountered. Further comparison of the two methods shows that the carbamate system requires twice the equilibrium time (about 100 hours) of the cyanide system. Therefore, suitable combinations of operating conditions and materials may improve the carbamate system to a point where it would be superior to the cyanide system.

Thermal Diffusion

Column Wire Heating by Alternating Current The use of alternating current for heating center wires of thermal diffusion columns is being studied. Effects of wire length, wire size, wire composition, weight attached to the wire, current strength, and temperature on the vibration patterns set up in the wire as a result of the current are being considered.

Nichrome V wire 1/16 inch in diameter and 36 inches long was mounted vertically on a wooden frame. The top of the wire was fastened to the framework, and the bottom was allowed to swing freely in a one-inch diameter, mercury-filled glass container. A short tungsten wire closed the circuit between the Nichrome V wire and the mercury pool. A direct current source was connected to the mercury pool and the top of the Nichrome wire through tungsten leads. Then the entire assembly was mounted atop a 55-gallon nonmagnetic stainless steel drum. A glass tube around the wire prevented air currents from moving the wire.

When 48 amperes at 24 volts was applied to the circuit, the Nichrome wire deflected away from the battery wire in the pool of mercury and toward the sides of the container. Reversing the polarity of the battery produced no significant change. The battery wire was then inserted through the bottom of the mercury container and aligned coaxially with the Nichrome wire. The deflection of the wire was similar, so a larger glass container was made for the mercury pool. This larger container did lessen the wire deflection; apparently, magnetic or electrostatic forces around the battery wire, and static electrical charges at the mercury-glass interface caused the wire to deflect to the glass wall. A deflection of about 1/16 inch was observed when the positive connection was in the mercury pool. The pool was rotated to see whether the battery wire and heated wire were aligned; there was no noticeable change in the deflection behavior.

The wire from the battery to the top of the nichrome wire was parallel to, and about six inches from, the Nichrome wire; a mutually repelling force between the two wires could cause a deflection on the wire. A current of 48 amperes running in opposite directions on the 36-inch long wire would have a mutually repelling force of 276 dynes between the wires. Therefore, it was concluded that the battery wire must be brought in perpendicular to the heated Nichrome V wire or that it must be magnetically shielded. It is believed that the repelling forces between the two wires when reinforced by the earth's magnetic field gave the 3/32-inch deflection mentioned above. When the polarity of the current was reversed, the force due to the earth's magnetic field was subtracted to give a 1/16-inch deflection. Grounding the mercury with the current on to remove the electrostatic charges built up at the glass-mercury interface had no effect on the deflection.

[10] Becker, *Z. Naturforsch.*, **7a**, 664 (1952).

Equation of the Steady State Vibration Electrical heating is the most common method used to heat the inner cylinder of a thermal diffusion column. The inner cylinder is located along the vertical axis of the column and is heated by passing a current either through the cylinder itself or through wires embedded in the cylinder. Generally, a magnetic field exists around the inner cylinder in the column due to the passage of current through the cylinder. If alternating current is used to heat the cylinder, the resulting magnetic force on the cylinder is a periodic function of time. In one type of column the inner cylinder is simply a wire, and this periodic force causes the wire to vibrate. To avoid this problem direct current is normally used in a hot wire column, but this substantially increases the construction and operating costs.

Another approach to the problem is to design the wire suspension system so that vibrations are damped out. Therefore, the equation describing the steady state vibrations of the wire was derived. In a hot-wire column the top of the wire is fastened to a rigid support; the wire is kept under a constant tension by a weight at the bottom of the wire. Supports which allow the wire to move vertically but not horizontally are placed at intervals along the wire. The lower end of the wire was selected as the origin of a coordinate system with the x-axis vertical and the y-axis horizontal.

Assume a flexible wire whose mass per unit length ρ is small compared with the attached mass m. The differential equation describing the motion of the wire is then the same as the differential equation for a vibrating string:

$$\frac{d^2y}{dt^2} + k\frac{dy}{dt} - \frac{1}{a^2}\frac{d^2y}{dx^2} = F \sin \omega t \qquad (1)$$

where

$a^2 = \rho/T$

$k = r/\rho$

$F = lB/\rho$

T = *the tension in the wire*

r = *a damping constant*

I = *the current in the wire*

ω = *the angular frequency of the alternating current*

B = *the flux density of the magnetic field perpendicular to the wire*

When all but the two end supports are ignored, the boundry conditions are:

$$y(O, t) = y(L, t) = O$$

In general, the initial displacement and velocity are arbitrary functions of x:

$$y(x, O) = f(x),\ y_t(x, o) = g(x)$$

The solution of Equation 1 consists of a transient term plus a steady state term. The transient term, which is the solution of Equation 1 when the right hand side is zero, is:

$$u(x,t) = e^{-(kt)/2} \sum_{n=o}^{\infty} (A_n \sin \lambda_n t + B_n \cos \lambda_n t) \sin \frac{n\pi x}{L} \qquad (2)$$

where

$$\lambda_n = \omega_n^2 - \frac{k}{4} > o$$

and

$$\omega_n = \frac{n\pi}{aL}$$

The constants A_n and B_n are determined by the initial conditions. This term approaches zero at large values of the time; hence, it makes no contribution to the steady state vibrations.

The steady state solution is a particular solution of Equation 1 and can be obtained in the following manner. Assume that the solution is:

$$v(x,t) = \sum_{n=1}^{\infty} A_n(t) \sin \frac{n\pi x}{L} \tag{3}$$

Substitute this expression into Equation 1, multiply the resulting equation by sin (mx)/L, and integrate from 0 to L . Since

$$\int_o^L \sin\frac{n\pi x}{L} \sin\frac{m\pi v}{L}\, dx = \begin{cases} 0, \text{ when } m \neq n \\ L/2, \text{ when } m = n \end{cases}$$

the following differential equation for A_n is obtained:

$$\ddot{A}_n + k\dot{A}_n + w_n^2 A_n = \frac{2(1 - \cos n\pi)}{n\pi} F \sin \omega t \tag{4}$$

Equation 4 is frequently encountered in problems of forced vibrations (e.g., in the problem of a forced harmonic oscillator), and its solution is:

$$A_n(t) = a_n \cos(\omega t - \phi_n)$$

where

$$a_n = \frac{2(\cos n\pi - 1) F}{n\pi [(\omega^2 - \omega_n^2)^2 + k^2\omega^2]^{1/2}} \tag{5}$$

$$\tan \phi_n = \frac{(\omega^2 - \omega_n^2)}{k\omega} \tag{6}$$

Thus, the equation describing the steady state vibrations of the wire is:

$$v(x,t) = \sum_{n=1}^{\infty} a_n \cos(\omega t - \phi_n) \sin \frac{n\pi x}{L} \tag{7}$$

ALPHA AND NEUTRON SOURCE DEVELOPMENT

Mound Laboratory is responsible for producing alpha and neutron sources, manufactured from polonium-210 and plutonium-239, which cannot be produced by American industry at the present time. The techniques of fabricating these unusual sources are being developed and publicized.

Alpha Sources

To date, the maximum amount of polonium which could be contained by electroplated gold was 5-10 millicuries per square centimeter. By a new procedure, however, the maximum polonium concentration may be increased by several orders of magnitude: freshly electroplated polonium was transferred wet from the polonium plating bath to a silver strike bath and then to a gold plating bath. Experiments to confirm this increase are continuing.

Neutron Sources

Several old PoBe neutron sources have recently been returned from the Martin-Marietta Corporation. Among them were two small sources prepared late in 1957. The sources are identified as N403 and N 404 and presently contain 0.15 and 0.21 millicuries, respectively, of polonium-210.

The polonium in N403 has been radiochemically removed, and alpha pulse height analysis has been carried out on a small aliquot of the purified solution. No alpha peaks characteristic of polonium-208 or polonium-209 were observed. Further work is in progress to determine the origin of the polonium used in the preparation of these sources.

Methods of analyzing elements and compounds are being developed to support other programs at Mound Laboratory. These methods include instrumental techniques and classical wet methods.

Beryllium Analysis by Gamma Activation

A method was developed for the destructive analysis of beryllium. A beryllium sample in solution is activated by a gamma source, and neutrons from the (γ, n) reaction in turn activate an indium foil detector which is then beta counted. The beta count is proportional to the neutron flux. Since the beryllium is dissolved, any beryllium-containing sample can be analyzed. The irradiation chamber in which the (γ, n) reaction occurs can be constructed in any convenient size.

The beryllium is dissolved in 40 milliliters of 1:3 sulfuric acid, and the solution is diluted to 100 milliliters. Forty milliliters of the diluted solution are put into the irradiation chamber. Then the chamber is placed in the center of a 40-gallon drum of paraffin and irradiated for one hour by an antimony-124 gamma source. An indium neutron detector is located at the bottom of the irradiation chamber.

The chamber is removed and the indium detector is counted at five-minute intervals for an hour.

From the beta count rate of the indium detector, a decay curve is plotted; the counting rate is extrapolated to the time at the end of irradiation. The rate is corrected for both the decay of the antimony-124 source and the weight of the indium foil detector. A number of analyses may be performed with the irradiation chamber if the foils used all have equal weights (± 0.005 gram); then the successive beta counts will be proportional to the beryllium sample weight.

A standard curve was determined by using spectrographic grade beryllium metal. The standard deviation for the analyses was ± 0.20 per cent. The results by gamma activation were an average 0.08 per cent below the values obtained by gravimetric analysis.

Low-level Krypton Counting

A sample of fission produced xenon containing an estimated 10^{-9} atom per cent krypton-85 was counted in the low level counting system. The results indicated that gases containing less than 10^{-12} atom per cent krypton-85 can be detected in this system; however, krypton is adsorbed on the walls of the proportional counting chamber during an experiment, and a purging procedure is being developed to keep the counter background at a constant rate.